[Research Paper] 대한금속 · 재료학회지 (*Korean J. Met. Mater.*), Vol. 58, No. 11 (2020) pp.793-797
DOI: 10.3365/KJMM.2020.58.11.793

Enhanced Optical and Electrical Properties of Ti Doped In_2O_3 thin Films Treated by Post-deposition Electron Beam Irradiation

Su-Hyeon Choe[1], Yun-Je Park[1], Yu-Sung Kim[2], Byung-Chul Cha[2], Sung-Bo Heo[3], Sungook Yoon[4], Young-Min Kong[1], and Daeil Kim[1,*]

[1]*School of Materials Science and Engineering, University of Ulsan, Ulsan 44776, Republic of Korea*
[2]*Advanced Forming Processes R&D Group, Korea Institute of Industrial Technology, Ulsan 44413, Republic of Korea*
[3]*Functional Components & Materials Group, Korea Institute of Industrial Technology, Yangsan 50635, Republic of Korea*
[4]*Welding and joining Research Dep't, Korea Shipbuilding & offshore Engineering, Ulsan 50635, Republic of Korea*

Abstract: Transparent and conductive Ti doped In_2O_3 (TIO) films were prepared on slide glass substrate using a radio frequency (RF) magnetron sputter and then subjected to Transparent and conductive Ti doped In_2O_3 (TIO) films were prepared on a glass slide substrate using radio frequency (RF) magnetron sputter. The film surface was then subjected to intense electron beam irradiation, to study the influence of incident energy on the visible transmittance and electrical resistivity of the films. All x-ray diffraction plots exhibited some diffraction peaks of the cubic bixbyite In_2O_3 (222), (400), (332), (431), (440), and (444) planes regardless of the electron irradiation energy, while the characteristic diffraction peak for crystalline TiO_2 did not appear even when irradiated at 1500 eV. In atomic force microscope analysis, the surface roughness of the as deposited TIO films was found to be 0.63 nm. As the electron irradiation energy was increased up to 1500 eV, the root mean square roughness decreased down to 0.36 nm. The films electron irradiated at 1500 eV showed higher visible transmittance of 83.2% and the lower resistivity of 6.4×10^{-4} Ωcm compared to the other films. From the electrical properties and optical band gap observation, it is supposed that the band gap shift is related to the carrier density. The band gap enlarged from 4.013 to 4.108 eV, along with an increase in carrier density from 9.82×10^{19} to 3.22×10^{20} cm^{-3}.

(Received April 23, 2020; Accepted September 2, 2020)

Keywords: TIO, magnetron sputtering, AFM, XRD, figure of merit

1. INTRODUCTION

Various indium oxide (In_2O_3) films doped with metals such as molybdenum (Mo) [1, 2] titanium (Ti) [3], zirconium (Zr) [4], tungsten (W) [5], and niobium (Nb) [6] exhibit high visible transmittance (≥ 80%) and low resistivity (≤ 1×10^{-3}cm), and have been applied in various optoelectrical devices including transparent thin film transistors (TTFT) and liquid crystal displays (LCD) [7, 8].

Among all the metal doped In_2O_3 films, Ti-doped In_2O_3 (TIO) and Mo-doped In_2O_3 (MIO) films have received attention because they exhibit high conductivity with rapid carrier mobility [9]. In a previous study, Y. Meng [10] reported a resistivity of 1.6×10^{-4} Ω cm for 4 at. % Mo-doped In_2O_3 films and asserted that the high conductivity was due to the substitution of In^{3+} by Mo^{6+}. In addition, T. Koida reported the enhanced near-infrared transparence of Zr doped In_2O_3 (ZIO) films, which had a resistivity of 2.6×10^{-4} Ω cm. The firms were deposited by the RF magnetron co-sputtering of In_2O_3 and $In_{1.9}Zr_{0.1}O_3$ targets, for thin film solar cells [4]. Also, R. K. Gupta prepared TIO films on sapphire substrate using KrF excimer laser deposition to examine the influence of substrate temperature on the opto-electrical properties of the films. They suggested the optimal temperature of 600 ºC, which assured higher carrier mobility than the other temperature conditions [11]. However, such high temperature is not recommended because it may restrict the type of flexible polymer substrate that can be used for bendable opto-electrical devices.

- 최수현·박윤제: 석사과정, 김유성·차병철·허성보·윤성욱: 연구원, 공영민·김대일: 교수
**Corresponding Author:* Daeil Kim
[Tel: +82-52-712-8066, E-mail: dkim84@ulsan.ac.kr]
Copyright ⓒ The Korean Institute of Metals and Materials

In this study, TIO films were deposited by the radio frequency (RF) magnetron sputtering of a Ti doped In_2O_3 target, and were then electron beam-irradiated to enhance the opto-electrical properties of the films. Electron beam irradiation with an optimal incident energy assures both low temperature grain growth and flat surface morphology, which will increase visible transmittance [12-14].

2. EXPERIMENTAL PROCEDURES

In this study, an RF (13.56 MHz) magnetron sputter with an electron irradiation system [12] was used to deposit the TIO thin films (thickness; 100 nm) on a slide glass substrate (size; 30 × 30 mm^2, Corning 2948) at room temperature. The chamber was evaluated to 5.5×10^{-7} Torr and then inert argon (Ar) was injected (10 sccm) to maintain a deposition pressure of 1.0×10^{-3} Torr. The TIO target was biased with RF 2.5 W/cm^2 for all depositions.

After deposition, we biased the RF power of 200 W on an inductively coupled plasma (ICP) antenna in an electron beam source and varied the electron irradiation energy from 300 to 1500 eV in a low vacuum of 1×10^{-5} Torr (Ar atmosphere). The variation in grain sizes related to optical transmittance and electrical resistivity was evaluated using an X-ray diffractometer (XRD, XPert-APD, Philips) at the Korea Basic Science Institute (KBSI), Daegu Center. The visible transmittance, sheet resistance, electrical properties, and chemical composition were observed by UV-visible spectrophotometry (Avaspec-2048L, Avantes), four point probe (Loresta-EP, Mitsubishi Chemical), Hall measurement system (HMS-3000, Ecopia) and energy dispersive spectrometer (EDS, JSM-6500F, JEOL), respectively. The bare glass had an optical transmittance of 92% in the visible wavelength region. In addition, the influence of electron irradiation on the surface roughness was investigated using an atomic force microscope (AFM, scan area; 3 × 3 μm^2, XE-100, Park Systems).

3. RESULTS AND DISCUSSION

In a previous study, Hest et al. deposited TIO films onto a glass substrate with a combinatorial sputtering system and investigated the relation between Ti doping rate (0-7 at. %) and carrier mobility [15]. It was demonstrated that films

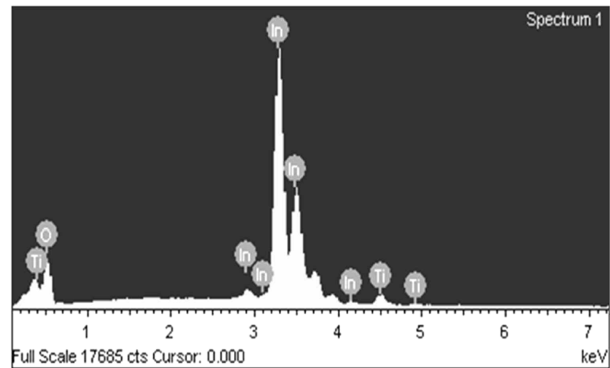

Fig. 1. The chemical composition of as deposited TIO film.

Table 1. The chemical composition of the target and film.

Element	Line	Target (at %)	Film (at %)
O	K	67.86	65.73
Ti	K	3.09	3.52
In	L	29.05	30.75

doped with 2.8 at. % of Ti showed excellent opto-electrical properties. Thus, we deposited TIO films by RF magnetron sputtering with 3.0 at. % Ti doped In_2O_3 target. Fig. 1 and Table 1 show the observed chemical composition of the films.

Fig. 2 shows the XRD patterns observed from the TIO films as a function of electron irradiation energy from 300 to 1500 eV. All of the XRD plots exhibited some diffraction

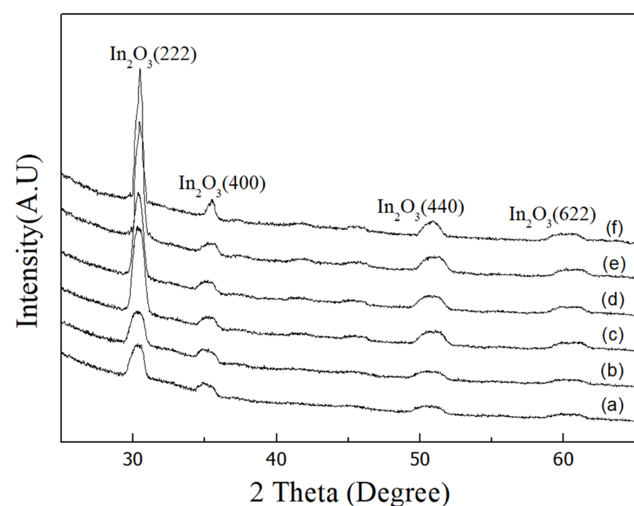

Fig. 2. The XRD pattern of the TIO films electron irradiated at different energy. (a) As deposition, (b) 300 eV, (c) 600 eV, (d) 900 eV, (e) 1200 eV, (f) 1500 eV.

Table 2. Grain size of In_2O_3 (222) plane in TIO films as a function of electron irradiated energy. (FWHM ; full width at half maximum)

Electron energy (eV)	2 Theta (Deg.)	FWHM (Deg.)	Grain Size (nm)
As deposition	30.40	1.0229	8.4
300	30.39	0.9019	9.1
600	30.38	0.7762	10.6
900	30.40	0.6601	12.5
1200	30.45	0.5772	14.3
1500	30.46	0.5279	15.6

peaks of the cubic bixbyite In_2O_3 (222), (400), (440), and (622) planes regardless of the electron irradiation energy, while the characteristic diffraction peak for crystalline TiO_2 did not appear, even at electron irradiation of 1500 eV. Table 2 shows the observed grain size of the In_2O_3 (222) plane using the Scherrer equation [16]. The average grain size with electron irradiation at 300, 600, 900, 1200, and 1500 eV were evaluated to be in the order of 9.1, 10.6, 12.5, 14.3 and 15.6 nm. It was concluded that the post-deposition electron irradiation was effective for enhancing the thin film crystallization.

Fig. 3 shows a surface image of the TIO films electron irradiated at different energies, with root mean square (RMS) roughness. The RMS roughness of the as deposited films was found to be 0.63 nm. As electron irradiation energy increased up to 1500 eV, the RMS roughness decreased down to 0.36 nm.

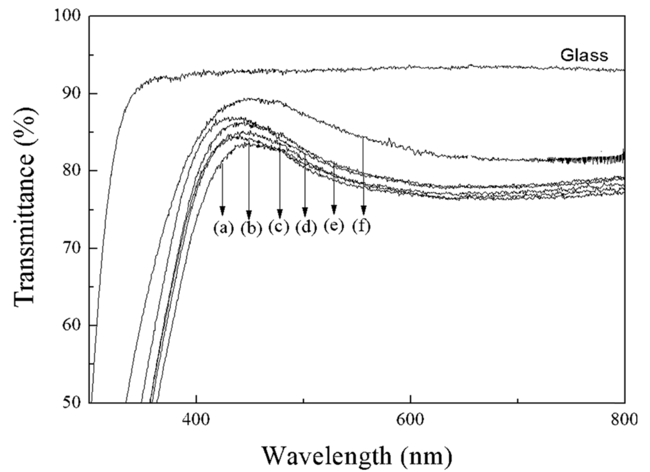

Fig. 4. The visible transmittance of the films electron irradiated at different energy. (a) As deposition 77.1%, (b) 300 eV 78.3%, (c) 600 eV 78.5%, (d) 900 eV 80.1%, (e) 1200 eV 80.5%, (f) 1500 eV 83.2%.

Fig. 4 shows the visible transmittance of the as deposited films, and after electron beam irradiation at different energies. The bare glass substrate had an optical transmittance of 93% in the visible wavelength region, while the as deposited film has a lower average visible transmittance of 77.1%. The visible transmittance was enhanced when the electron irradiation energy increased. The average visible transmittance of the films electron-irradiated at 1500 eV was 83.2%. From XRD and AFM observations, it was found that the increased

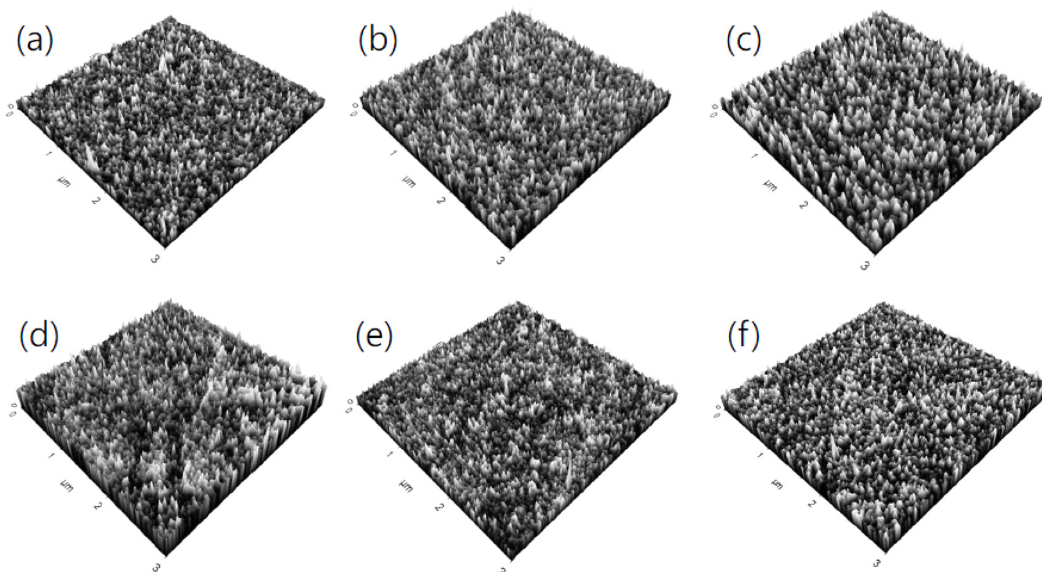

Fig. 3. Surface image and RMS roughness of the films electron irradiated at different energy. (a) As deposition, 0.65 nm, (b) 300 eV, 0.61 nm, (c) 600 eV, 0.51 nm, (d) 900 eV, 0.43 nm, (e) 1200 eV, 0.39 nm. (f) 1500 eV, 0.36 nm.

Table 3. The electrical properties of TIO films as a function of electron irradiation energy.

Electron energy (eV)	Carrier Density (cm^{-3})	Mobility (cm^2/vs)	Resistivity (Ωcm)
As deposition	9.82×10^{19}	21.5	2.9×10^{-3}
300	1.06×10^{20}	22.6	2.2×10^{-3}
600	1.24×10^{20}	24.7	2.0×10^{-3}
900	2.63×10^{20}	25.7	9.2×10^{-4}
1200	3.05×10^{20}	27.1	7.5×10^{-4}
1500	3.22×10^{20}	30.1	6.4×10^{-4}

Table 4. The electrical properties of impurity doped In_2O3 thin films.

Dopant	Carrier density (cm^{-3})	Mobility (cm^2/vs)	Resistivity (Ωcm)	Reference
Mo	4.9×10^{20}	17.2	7.3×10^{-4}	2
W	2.4×10^{20}	26.0	1.0×10^{-3}	5
Zr	1.0×10^{20}	110	5.7×10^{-4}	4
Ti	1.0×10^{20}	120	5.2×10^{-4}	14
Ti	4.9×10^{20}	17.0	7.3×10^{-4}	15
Ti	3.2×10^{20}	30.1	6.4×10^{-4}	This study

visible transmittance of the TIO films could be attributed to a flatter surface and larger grain size, induced by the post-deposition electron irradiation.

Table 3 shows the dependence of electrical resistivity, carrier density, and mobility on electron irradiation energy. The TIO films electron irradiated at 1500 eV show a higher carrier density of 3.22×10^{20} cm^{-3}. Both carrier density and carrier mobility were enhanced by increases in the electron incident energy. The highest mobility of 30.1 cm^2/Vs was observed for TIO films electron irradiated at 1500 eV. The decrease in resistivity (6.4×10^{-4} Ωcm) with increasing electron irradiation energy was attributed to the enlargement in grain size, as shown in Table 1.

Table 4 shows the compared electrical properties of some impurity doped In_2O_3 thin films. The Ti doped films showed relatively low resistivity from 5.2×10^{-4} Ωcm to 7.3×10^{-4} Ωcm, depending on the deposition method and substrate temperature conditions. In Table 3, even though some Ti and Zr doped films showed lower resistivity than the TIO films prepared in this study, those films were deposited at a relatively high substrate temperature, of 500 °C for the Ti doped films [17] and 650 °C for the Zr doped films [4].

Fig. 5 shows a plot of $(\alpha h\nu)^2$ of the TIO films as a function of the photon energy. The absorption coefficient (α) is evaluated from Eq. (1) [18]:

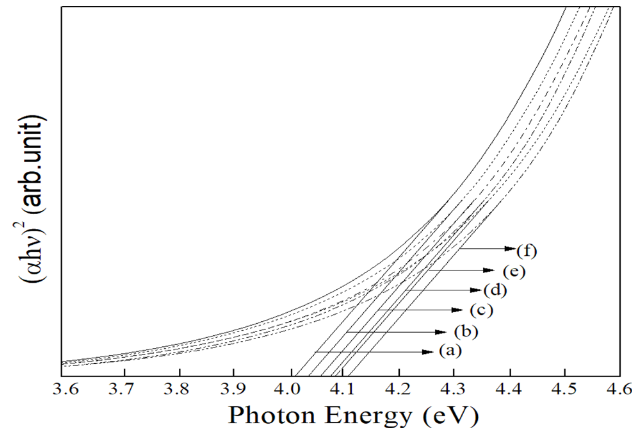

Fig. 5. Plots of $(\alpha h\nu)^2$ as a function of the photon energy(hν) for TIO thin films electron irradiated at different energy. (a) As deposition, (b) 300 eV, (c) 600 eV, (d) 900 eV, (e) 1200 eV, (f) 1500 eV.

$$\alpha = (1/t) \ln (1/T) \quad (1)$$

where t is the thickness and T is the visible transmittance. The Tauc formula in Eq. (2) shows the relationship between the optical absorption coefficient (α) and the optical band gap (Eg) [19]:

$$(\alpha h\nu)^2 = A(h\nu - Eg) \quad (2)$$

where hν is the photon energy and A is the absorption edge width parameter. In Fig. 5, the optical band gap increased from 4.013 (at deposition) to 4.108 eV as the electron energy was increased to 1500 eV.

Table 5 shows the carrier density and optical band gap of

Table 5. The carrier density and optical band gap of TIO films as a function of electron irradiation energy.

Electron energy (eV)	Carrier density ($\times 10^{19}$ cm^{-3})	Optical band gap (eV)
As deposition	9.82	4.013
300	10.6	4.034
600	12.4	4.054
900	26.3	4.078
1200	30.5	4.086
1500	32.2	4.108

the TIO films as a function of the electron irradiation energy. From the observed electrical properties and optical band gap, it is concluded that the optical band gap shift is related to the carrier density of the films [20,21]. The band gap was enhanced from 4.013 to 4.108 eV, while the carrier density increased from 9.8×10^{19} (at deposition) to 3.22×10^{20} cm^{-3} (at 1500 eV).

4. CONCLUSIONS

Conductive and transparent TIO films were prepared on glass slide substrates using RF magnetron sputtering and then electron beam irradiation, to study the influence of incident electron energy on the visible transmittance, optical band gap, and electrical resistivity of the films. XRD patterns and AFM images showed that the crystallite size increased with electron irradiation energy, and the electron irradiated films at 1500 eV showed the lowest RMS roughness of 0.36 nm. The decrease in resistivity (6.4×10^{-4} Ωcm) with increasing electron irradiation energy was attributed to the enhanced crystallinity and surface flatness of the films. The results demonstrated that electron beam irradiation effectively improved the optical and electrical performances of the TIO thin films.

Acknowledgement

This work was supported by the 2020 Research Fund of University of Ulsan.

REFERENCES

1. D. J. Seo and S. H. Park, *Physica.* B **357**, 420 (2005).
2. R. Hashimoto, Y. Abe, and T. Nakada, *Appl. Phys. Express* **1**, 015002 (2008).
3. T. Koida and M. Kondo, *Appl. Phys. lett*. **89**, 082104 (2006).
4. T. Koida and M. Kondo, *J. Appl. Phys.* **101**, 063705 (2007).
5. D. R. Acosta and A. I. Martínez, *Thin Solid Films* **515**, 8432 (2007).
6. R. K. Gupta, K. Ghosh, R. Patel, S. R. Mishra, and P. K. Kahol, *Mater. Chem. Phys*. **112**, 136 (2008).
7. S. B. Koo, C. M. Lee, S. J. Kwon, J. M. Jeon, J. Y. Hur, and H. K. Lee, *Met. Mater. Int.* **25**, 117 (2019).
8. H. S. Kim and S. J. Kim, *Korean J. Met. Mater*. **57**, 84 (2019).
9. D. Kim, B. Kim, and H. Kim, *Thin Solid Films* **547**, 225 (2013).
10. Y. Meng, X. Yang, H. Chen, J. Shen, Y. Jiang, Z. Zhang, and Z. Hua, *J. Vac. Sci. Technol*. *A* **20**, 288 (2002).
11. R. K. Gupta, K. Ghosh, S. R. Mishra, and P.K. Kahol, *Mater. Lett*. **62**, 1033 (2008).
12. Y. S. Kim, J. Y. Choi , Y. J. park, S. H. Choe, B. C. Cha, Y. M. Kong , and D. Kim, *Korean J. Met. Mater*. **58**, 190 (2020).
13. C. H. Hong, Y. J. Jo, H. A. Kim, I. H. Lee, and J. S. Kwak, *Thin Solid Films* **519**, 6829 (2011).
14. Y. Li, L. Han, and X. Kong, *Mater. Sci. Eng.* **677**, 022066 (2019).
15. M. F. A. M. van Hest, M. S. Dabney, J. D. Perkins, and D. S. Ginley, *Appl. Phys. Lett*. **87**, 032111 (2005).
16. T. K. Gong, S. B. Heo, and D. Kim, *Ceram. Inter*. 42, 12341 (2016).
17. R. Groth, *Phys. Status Solidi* **14**, 69 (1966).
18. S. Peng, T. Yao, Y. Yang, K. Zhang, J. Jiang, K. Jin, G. Li, X. Cao, G. Xu, and Y. Wang, *Physica B* **503**, 111 (2016).
19. J. Tauc, *Mater. Res. Bull* **3**, 37 (1968).
20. W. H. Jo and D. Choi, *Korean J. Met. Mater*. **57**, 91 (2019).
21. E. Jeong, G.-H. Lee, Y.-R. Cho, and J. Yun, *Korean J. Met. Mater*. **57**, 316 (2019).